Dielectric Study of Molecular Mobility in Poly(propylene-graft-maleic anhydride)/Clay Nanocomposites

ARTICLE *in* MACROMOLECULES · APRIL 2005

Impact Factor: 5.8 · DOI: 10.1021/ma048315c

Dielectric Study of Molecular Mobility in Poly(propylene-*graft*-maleic anhydride)/Clay Nanocomposites

Martin Böhning,* Harald Goering, Andreas Fritz,† Klaus-W. Brzezinka, Gamal Turky,‡ Andreas Schönhals, and Bernhard Schartel

Federal Institute for Materials Research and Testing (BAM), Unter den Eichen 87, D-12200 Berlin, Germany

Received August 17, 2004; Revised Manuscript Received January 20, 2005

ABSTRACT: Polymer/clay nanocomposite materials based on poly(propylene-*graft*-maleic anhydride) (PPgMAH) and two different organophilic modified clays were investigated by dielectric relaxation spectroscopy (DRS). In contrast to ungrafted polypropylene (PP), PPgMAH shows a dielectrically active relaxation process which can be assigned to localized fluctuations of the polar maleic anhydride groups. Its relaxation rate exhibits an unusual temperature dependence, which could be attributed to a redistribution of water molecules in the polymeric matrix. This is confirmed by a combination of Raman spectroscopy and thermogravimetric experiments (TGA) with real-time dielectric measurements under controlled atmospheres. In the nanocomposites this relaxation process is shifted to higher frequencies up to 3 orders of magnitude compared to the unfilled polymer. This indicates a significantly enhanced molecular mobility in the interfacial regions. In the nanocomposite materials a separate high-temperature process due to Maxwell−Wagner−Sillars (MWS) polarization was observed. The time constant of this MWS process can be correlated with characteristic length scales in nanocomposites and therefore provides additional information on dispersion and delamination/exfoliation of clay platelets in these materials. These properties also influence the diffusivity of the water molecules as revealed by real-time dielectric investigations.

1. Introduction

Over the past decade polymer-based nanocomposites gained rapidly increasing interest due to their favorable and often unique combination of properties. Within this class of materials nanocomposites formed by dispersion of layered silicates (clays) in a polymeric matrix represent one of the most important type because, due to their high aspect ratio, silicate nanolayers seem to be favorable filler particles in order to attain mechanical reinforcement or formation of barrier structures which reduce the diffusive transport of small penetrant molecules (i.e., gases or vapors).[1,2] In addition to that, such polymer/layered silicate (PLS) nanocomposites often possess improved thermal and fire-retardant properties.[3−5]

In clay structures of the montmorillonite (MMT) type the single silicate layers have a thickness of about 1 nm and typically lateral dimensions of several hundred nanometers up to micrometers. These layers are arranged in stacks with regular interstices called interlayer galleries. To enable the formation of nanocomposites, i.e., compatibility with polymeric matrices and intercalation of polymer chains in these interlayer galleries, organomodified clay minerals are used in which the counterions of the silicate layers (typically Na^+, Li^+, Ca^{2+}) situated in the interstitial regions were exchanged with bulky alkylammonium ions. Meanwhile, such organomodified clays are available commercially in several variations, tailor-made for different applications, and compatible with different polymeric materials. Therefore, process monitoring during preparation and characterization of the resulting nanocomposite materials is of increasing importance.

Because of the small dimensions of the filler particles and the resulting high surface-to-volume ratio, nanocomposites typically have, even at low filler concentrations, a high fraction of interfacial regions (interphase) with a major influence on the physical properties and therefore on the material performance.[6] In this study dielectric relaxation spectroscopy (DRS)[7] was used to investigate the molecular mobility in such systems, which may be utilized as an indicator for the characterization of nanocomposite materials with regard to nanoparticle dispersion and filler/matrix interactions.

From a scientific point of view such nanocomposites give rise to questions concerning the dynamic behavior of the polymeric matrix, especially of those parts being preferentially located in the interfacial regions. On one hand, a close contact of polymer segments to a rigid inorganic structure may slow down their dynamics[8,9] where extent and spatial range of this influence should depend on their intermolecular interactions as well as their chain stiffness.[10,11] On the other hand, dimensional restrictions in the nanometer range may have an effect on the cooperativity of motional processes of the polymer (e.g., the glass transition, often referred to as confinement effect[12,13]) or induce changes in the local free volume distribution,[14,15] possibly leading to enhanced molecular mobility. A comprehensive discussion of such a complex behavior concerning the molecular mobility in polymer/layered silicate nanocomposites resulting from the interplay between intercalation of polymer chains into interlayer galleries of the silicate structure, exfoliation of silicate layers, and the interaction strength between silicate surface and polymer chain can be found in ref 16 (and references therein). Such details of the

† Current address: TFH Wildau, University of Applied Sciences, Department of Engineering, D-15745 Wildau, Germany.
‡ Current address: National Research Center, Physics Department, Dokki, Cairo, 12622 Giza, Egypt.
* Corresponding author: Tel +49 30/8104-3109; Fax +49 30/8104-1637; e-mail Martin.Boehning@bam.de.

10.1021/ma048315c CCC: $30.25
Published on Web 03/11/2005

local polymer structure and dynamics in the interfacial regions adjacent to rigid inorganic fillers have also been identified to be of decisive importance for the development of mixed-matrix membrane materials for gas separation.[17]

From a practical point of view, the present study may also contribute to the development of methods for handy and reliable assessment of nanocomposites and nanoparticle dispersion as well as silicate layer exfoliation. Based on dielectric relaxation spectroscopy, approaches for on-line monitoring of nanocomposite processing have been developed as reported by Bur et al.[18−20] Other methods for the determination of the state of nanodispersion rely on rheology[21] or the determination of characteristic proton relaxation times by solid-state NMR.[22] A better understanding of structure and dynamic behavior of the extended interphase fraction in nanocomposites should also significantly improve the specific development of such materials, especially for more sophisticated applications in optics, microelectronics, and the field of functional materials.

Particular interest to attain improved material properties by incorporation of nanofillers exists for polymers with practical relevance and large commercial importance but insufficient material performance for certain applications, such as polypropylene (PP). Preparation of PP/clay nanocomposites by melt compounding requires in addition to the use of suitable organomodified clays an oligomeric or polymeric compatibilizer.[23,24] For the latter, PP functionalized with polar groups can be employed and most frequently poly(propylene-*graft*-maleic anhydride) (PPgMAH) is used for this purpose.

With respect to molecular relaxation processes in polymeric materials DRS is only sensitive to fluctuations of those parts of the polymer which possess a permanent dipole moment. For the investigation of clay nanoparticles in a polymeric matrix with a low content of grafted polar groups, here the 0.6 wt % grafted maleic anhydride (MAH) in PP, this can be regarded as an unique advantage due to the fact that the dielectrically "visible" polar MAH groups—acting as a compatibilizer—are expected to be preferentially situated near the surface of the silicate layers or inside the interlayer galleries of the clay filler and thus act as a specific local probe of the interface regions. The overall segmental dynamics of the polymer matrix (modified PP) cannot be studied directly by this method due to the low concentration and irregular distribution of the MAH units (although their localized fluctuations may be dependent on the segmental mobility as these groups are directly grafted to the polymer chain; cf. section 4.1). Therefore, a direct comparison to studies addressing the dielectric relaxation behavior of an unmodified homopolymer in a clay nanocomposite[25,26] might prove difficult as there also the influence on the segmental dynamics of the polymer chain is directly detected. Furthermore, ionic conductivity and polarization effects caused by (partial) blocking of mobile charge carriers in inhomogeneous materials (Maxwell−Wager−Sillars polarization) can strongly influence the DRS measurements. Also, the inorganic filler structure (clay) as well as the bulky organic cations may be considered as components affecting the dielectric spectra.

In the course of the investigations a significant influence of sorbed water molecules on the behavior of the matrix polymer was found. So in addition to conventional dielectric relaxation spectroscopy, real-time DRS experiments under controlled atmosphere were carried out. Conventional DRS consists of recording the frequency-dependent dielectric behavior at constant temperatures which are changed in a stepwise manner. For the real-time DRS experiments the frequency-dependent dielectric properties were recorded successively after well-defined time intervals following a change of the atmosphere to which the sample was exposed at one constant temperature. These investigations were supplemented by gravimetric experiments and Raman spectroscopy.

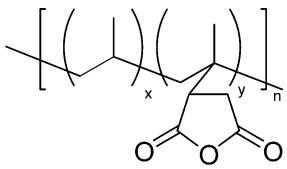

Figure 1. General structure of poly(propylene-*graft*-maleic anhydride) ($y \sim 0.6$ wt % for the polymer used in this study).

2. Materials

The preparation of the investigated nanocomposites is described in detail in a previous study by Tidjani et al.,[27] where also a discussion of the influence of the presence of oxygen during melt-blending/preparation—causing a partial degradation of the organic cations used to modify one the clay fillers (30B)—on the resulting PLS nanocomposites as well as their thermal stability is included.

Poly(propylene-*graft*-maleic anhydride) (PPgMAH, polypropylene with ca. 0.6 wt % grafted maleic anhydride (MAH)) was purchased from Sigma-Aldrich (mp 152 °C, melt index 115 g/10 min at 190 °C/2.16 kg). Its chemical structure is sketched in Figure 1.

Two different organophilic modified montmorillonite clays, Nanomer I28E and Cloisite 30B, obtained from Nanocor, Inc., and Southern Clay Products, Inc., respectively, were used as filler particles. In the following text these two clay types are referred to as I28E and 30B.

These montmorillonite clays are designed to facilitate the intercalation of polymer chains. Therefore, they are modified with ternary alkylammonium ions (R_4N^+) in the interlayer galleries in order to widen the distance between the individual silicate layers and make their surface more hydrophobic. I28E contains octadecyltrimethylammonium ions (denoted as OD3MA) whereas for 30B the bulky ammonium ion (denoted as MT2EtOH) contains one methyl group, two 2-hydroxyethyl groups, and one C_{16}/C_{18} hydrocarbon rest (denoted "tallow").

Nanocomposites with a clay content of 5.0 wt % were prepared by melt blending at 453 K in the presence of air using a Brabender mixer.[27] Films of about 200 μm thickness were prepared at temperatures between 433 and 453 K in a hydraulic press. The degree of crystallinity (X_C) and the melting temperature (T_M) were determined by DSC and differ only slightly for the materials investigated ($X_C^{PP} = 40\%$ and $T_M = 437$ K for PPgMAH, $X_C^{PP} = 47\%$ and $T_M = 435$ K for PPgMAH/30B, $X_C^{PP} = 48\%$ and $T_M = 436$ K for PPgMAH/I28E).[27] It can be therefore assumed that also in the composite materials these properties are mainly determined only by the matrix in which crystallinity might be predominantly influenced by the content of grafted MAH groups.

The formation of layered silicate nanocomposites can be regarded as a multistage process. Upon adding of the

clay particles to the polymer melt at first a microcomposite containing agglomerates of stacked silicate layers (tactoids) is formed. During further mixing the stage of an intercalated nanocomposite may be reached where polymer chains have entered the galleries between the silicate layers. Finally, a true exfoliated nanocomposite is obtained when the stacks of silicate layers delaminate and individual layers are dispersed in the polymer matrix. The formation of intercalated and exfoliated clay nanocomposites may partially depend on the preparation conditions (processing time or mechanical influences such as shear), but it is primarily governed by thermodynamic factors, i.e., the interactions between the polymer and the silicate surfaces.[2,28,29] The latter can be influenced by the nature of the organophilic cations in the clay and modifications of the host polymer or use of a compatibilizer.

The state of organoclay dispersion has been investigated by transmission electron microscopy (TEM) using a Philips CM20 at 200 kV. Samples were prepared using a MT-7000 Ultra-mitrotome (RMC, Tucson, AZ). The two micrographs shown in Figure 2 clearly reveal the differences between the two materials.

Both systems still contain larger clay units, but compared to PPgMAH/30B the PPgMAH/I28E material contains more separate exfoliated layers of the organoclay filler which are also much more homogeneously dispersed in the polymer matrix.

So the investigated samples represent both a material with poorly dispersed clay platelets (PPgMAH/30B) and a well-dispersed largely homogeneous nanocomposite system (PPgMAH/I28E). They were investigated in comparison to the pure matrix polymer (PPgMAH). The poorer dispersion and lower degree of intercalation of polymer chains in the first system have been ascribed to a partial degradation of organic cations (MT2EtOH) during processing in the presence of air. This finding is based on the comparison of X-ray diffraction patterns of PPgMAH/30B with the respective organoclay powder which reveals a significant decrease of the observed d spacing. The TEM images of the resulting composite materials show large unperturbed clay stacks and only a marginal degree of intercalation/delamination. In contrast to this, the PPgMAH/I28E system leads to well-dispersed, largely exfoliated silicate layers as revealed by TEM images and a vanishing d spacing peak of the regularly stacked silicate layers in the X-ray diffraction pattern.[27] It has to be noted that all materials under investigation have to be regarded as multicomponent blends in which all stages of composite formation (tactoid, intercalated, and exfoliated) are present at different fractions. So in the poorly dispersed nanocomposite system (PPgMAH/30B) the tactoid state dominates whereas in the well-dispersed system (PPgMAH/I28E) the intercalated/exfoliated state predominantly determines the properties of the composite material.

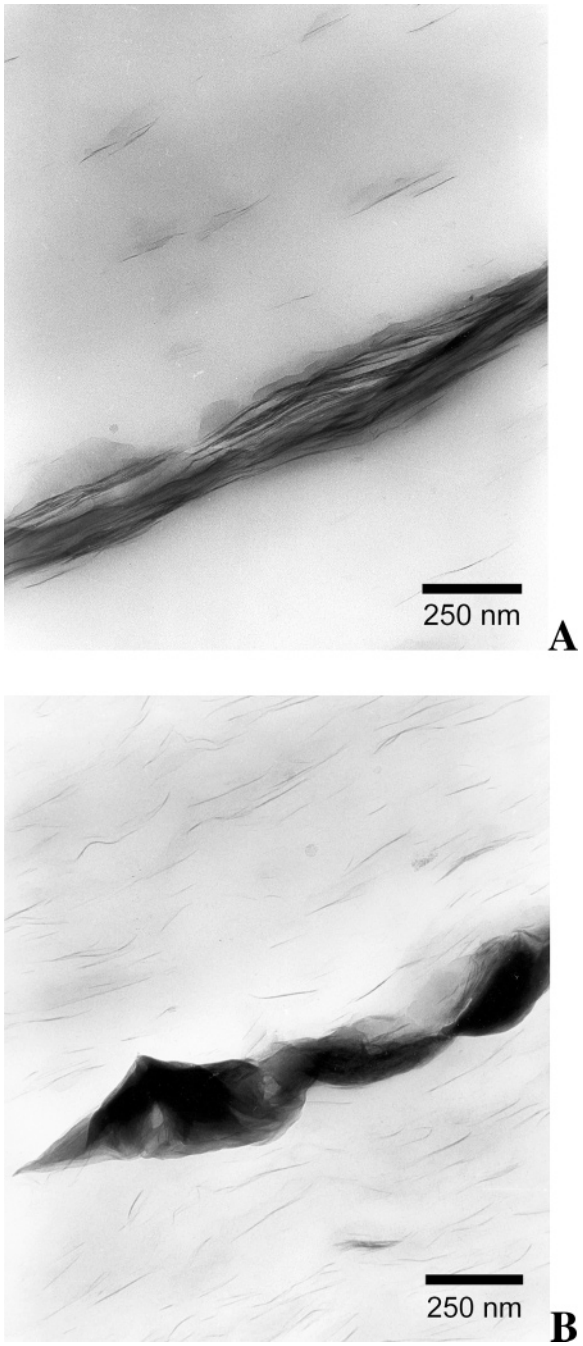

Figure 2. Transmission electron micrographs of the nanocomposite materials under investigation: PPgMAH/30B (A) and PPgMAH/I28E (B).

3. Experimental Section

3.1. Dielectric Relaxation Spectroscopy (DRS). DRS was performed by measurement of the complex dielectric function

$$\epsilon^*(f) = \epsilon'(f) - i\epsilon''(f) \quad (1)$$

where f is the frequency, ϵ' is the real part, ϵ'' is the imaginary or loss part, and $i = \sqrt{-1}$ using two different setups.

3.1.1. Conventional DRS. For the conventional measurements covering a frequency range from 10^{-1} to 10^{6} Hz a frequency response analyzer Solartron/Schlumberger FRA 1260 connected to a buffer amplifier of variable gain (Chelsea dielectric interface) was used. Samples of about 200 μm thickness and 20 mm diameter were investigated between gold-plated stainless steel electrodes (plate capacitor geometry). The temperature of the sample was controlled by a custom-made gas jet heating system operated with liquid nitrogen. Before each frequency sweep the sample was thermally equilibrated at the selected temperature (ranging from 195 to 370 K) with a stability of 0.05 K.

3.1.2. Real-Time DRS. Real-time measurements in the frequency range from 10^{-2} to 10^{5} Hz under controlled atmospheres were carried out using a lock-in amplifier Stanford Research SR810 interfaced with a Novocontrol BDC broadband dielectric converter. The sample holder (identical geometry as for the conventional temperature-dependent measurements) was placed in a stainless steel vessel and connected via

vacuum-tight coaxial electrical feedthroughs (Ceramaseal BNC, $^3/_8$ in. NPT). Via a three-way valve, the vessel could be connected to a vacuum system (Pfeiffer Vacuum TSH-071E turbomolecular pump system) and a gas supply (dry synthetic air) or room atmosphere. The experiments were performed at room temperature (298 ± 2 K). It should be noted that in the setup used here the massive stainless steel vessel (originally designed for high-pressure applications up to 50 bar), utilized to provide a controlled atmosphere during the real-time dielectric experiments—due to its huge heat capacity—does not allow to cover the temperature range or reach reasonable heating rates in order to perform conventional DRS measurements.

Both measurements were analyzed with respect to the frequency of maximal dielectric loss f_p (mean relaxation rate) and the dielectric relaxation strength $\Delta\epsilon$ by fitting the Havriliak−Negami (HN) function (eq 2) to the data ($\omega = 2\pi f$).

$$\epsilon^*_{HN} = \epsilon_\infty + \frac{\Delta\epsilon}{(1 + (i\omega\tau_{HN})^\beta)^\gamma} \quad (2)$$

where $\epsilon_\infty = \lim_{\omega\to\infty} \epsilon'(\omega)$, τ_{HN} is a relaxation time corresponding to f_p, and β and γ are shape parameters describing symmetric and asymmetric broadening, respectively; for further details see ref 7. When necessary, the influences of other processes affecting the dielectric relaxation peak (such as Maxwell−Wagner−Sillars polarization or conductivity) were taken into account for the analysis by standard procedures.[7]

3.3. Gravimetric Experiments. 3.3.1. Gravimetry (Dry Atmosphere). Gravimetric experiments to estimate the water content of the matrix polymer (PPgMAH) were carried out under controlled atmosphere in contact with silica gel as desiccant using a high-pressure microbalance (Sartorius 4406, 100 mg range, 1 μg resolution) with temperature control.

3.3.2. Thermogravimetric Analysis (TGA). Also, TGA was employed to determine mass changes at elevated temperatures up to 413 K using a Rheometric Scientific STA 1000.

3.4. Raman Spectroscopy. Raman spectra were collected in backscattering geometry at room temperature in ambient atmosphere using a Dilor XY spectrometer equipped with a liquid nitrogen-cooled multichannel detector. The samples were excited with an argon ion laser (λ = 514.5 nm), which was focused on the sample to a spot of about 2 μm diameter. The exciting laser power was 10 mW, yielding a power density at the sample surface of 1 mW μm^{-2}. Spectra were recorded using an integration time of 100 s (2-fold accumulation) with a spectral resolution of 1 cm^{-1}.

3.5. Dynamic Mechanical Analysis. To determine the glass transition temperature (T_G) of the pure matrix polymer PPgMAH as well as the two nanocomposites, dynamic mechanical analysis (DMA) was employed because T_G was not clearly detectable by DSC measurements. The DMA experiments were carried out in the temperature range from 193 to 413 K using a Myrenne torsional pendulum at 1 Hz. The film samples of 0.5 mm thickness (10 mm width and 50 mm gage length) for DMA was prepared by the same procedure as the thinner samples used for the dielectric investigations.

4. Results

To describe the changes of the molecular mobility due to the influence of incorporated clay particles at first the results for the pure polymer matrix (PPgMAH) will be presented. Results for the two nanocomposites will then be discussed in comparison to that taking into account the effect of sorbed water as characterized by gravimetric experiments and Raman spectroscopy for PPgMAH.

4.1. Conventional DRS: PPgMAH. The dielectric response of the unfilled PPgMAH matrix is due to fluctuations of the grafted maleic anhydride groups being the only structural units present therein which exhibit a permanent dipole moment. Figure 3 shows a comparison of dielectric spectra of PPgMAH with ungrafted polypropylene (PP) which shows, as expected, no dielectrically active relaxation process.

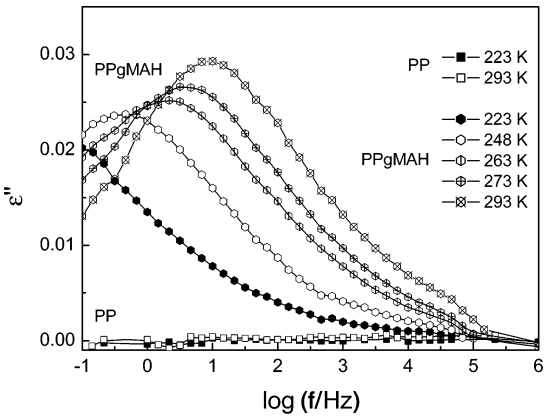

Figure 3. Comparison of dielectric spectra of polypropylene (PP) and poly(propylene-*graft*-maleic anhydride) (PPgMAH).

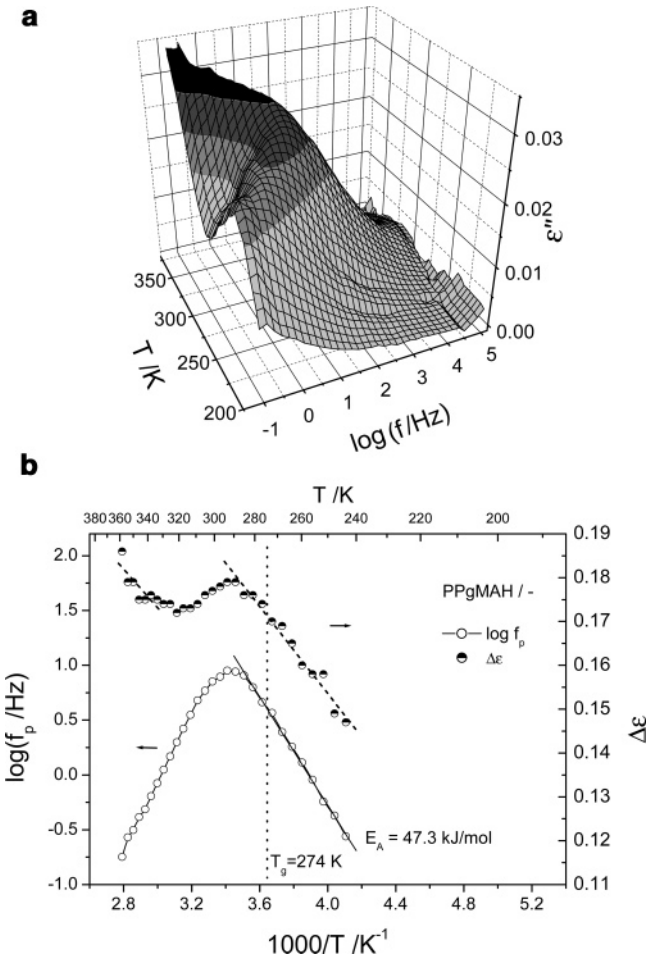

Figure 4. (a) Three-dimensional representation of the dielectric loss ϵ'' of PPgMAH vs frequency and temperature (conventional DRS). (b) Frequency of maximal dielectric loss f_p and dielectric relaxation strength $\Delta\epsilon$ of PPgMAH vs $1/T$ (conventional DRS, the dotted line indicates the glass transition temperature T_g as determined by DMA).

For PPgMAH conventional DRS reveals one relaxation process. Results are presented as a three-dimensional representation in Figure 4a. For temperatures up to 293 K an Arrhenius-like shift of the relaxation rate f_p with an activation energy of E_A = 47.3 kJ/mol is observed (Figure 4b). This is expected for a relaxation

process due to local molecular fluctuations (β-relaxation). The exact motional process cannot be deduced from this experiment, but it clearly is related to the presence of polar MAH goups which are rigidly bonded to the polymer chains. Surprisingly, above 293 K the frequency of maximal dielectric loss shifts to lower values again with further increasing temperature. This can already be clearly seen from the raw data (Figure 4a, see also Figure 12). It has to be noted that no α-process (corresponding to the segmental dynamics connected with the glass transition) could be detected which is possibly due to the low concentration of grafted MAH groups bearing the dipole moment and their irregular distribution along the PP chains.

To further analyze the unusual behavior of the observed relaxation process, the temperature dependence of the dielectric relaxation strength $\Delta\epsilon$ is taken into consideration. The relation of $\Delta\epsilon$ to the mean-squared dipole moment μ^2 according to the Debye−Fröhlich−Kirkwood theory is given by eq 3[30]

$$\Delta\epsilon = \epsilon_S - \epsilon_\infty = \frac{1}{3\epsilon_0} Fg \frac{\mu^2}{k_B T} \frac{N}{V} \tag{3}$$

where $\epsilon_S = \lim_{\omega\to 0} \epsilon'(\omega)$, $\epsilon_\infty = \lim_{\omega\to\infty} \epsilon'(\omega)$, N/V is the number density of dipoles, k_B is the Boltzmann constant, and T is the temperature. Furthermore, the dielectric relaxation strength is affected by the Kirkwood/Fröhlich correlation factor g, describing the interactions of a selected dipole with dipoles in its immediate vicinity. The influence of the unspecific Onsager factor F, which considers internal field effects in condensed systems, can be neglected for the systems under investigation.[7]

From the data shown in Figure 4b it can be seen that simultaneous to the shift of f_p to lower values with increasing temperature the dielectric strength $\Delta\epsilon$ also shows a nonmonotonic variation with temperature. The general increase of $\Delta\epsilon$ with increasing temperature is typically observed for β-relaxations in polymeric systems.[31] It is usually ascribed to an enhanced mobility of the molecular dipoles mainly caused by a higher mobility of the surrounding matrix or by an increase of the number density of dipoles. The decrease of $\Delta\epsilon$ observed in the temperature interval between 293 K and about 323 K may be ascribed to changes of the effective dipole moment, i.e., the Kirkwood−Fröhlich correlation factor g,[30] due to changes of the local molecular environment of the dipoles.

It has to be noted that $\Delta\epsilon$ has been determined only for those peaks in the dielectric spectra for which the peak maximum was clearly discernible. Furthermore, in order to minimize the error the analysis was performed using a symmetric relaxation function ($\gamma = 1$, eq 2) as for a β-relaxation a symmetric peak has to be expected.[31] So the error of the $\Delta\epsilon$ values in Figure 4b (as well as in Figures 10 and 11) can be estimated to 2−3%. Therefore, a quantitative assessment might be arguable in these cases, but despite the error a change of the dielectric strength $\Delta\epsilon$ is obvious, which supports the experimental evidence of the influence of sorbed water on the relaxation behavior.

4.2. Dynamic Mechanical Analysis. The temperature range where the suggested changes of the local environment of the MAH groups (which cause the unusual dielectric behavior described above) occur might be due to changes of the overall mobility of the polymer matrix (i.e., the segmental relaxations connected with the glass transition). As no corresponding α-process was detected in the dielectric spectra, the glass transition temperature of PPgMAH was measured by dynamic mechanical analysis (DMA), as shown in Figure 5.

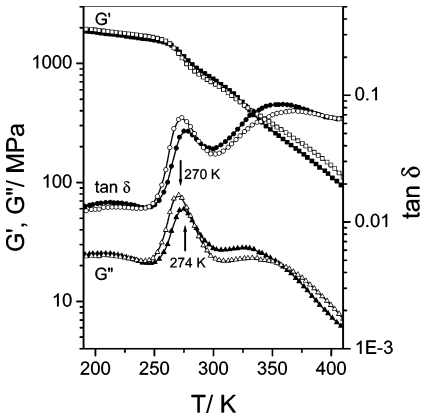

Figure 5. DMA (torsional pendulum, 1 Hz) of PPgMAH: shear modulus G', G'', and mechanical loss tan δ (solid symbols: first heating run; open symbols: second heating run).

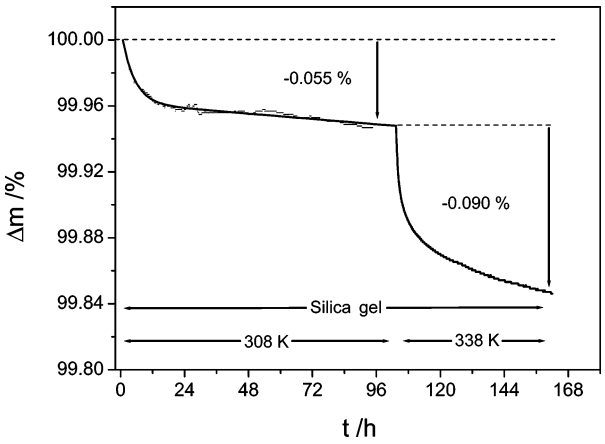

Figure 6. Weight change Δm of PPgMAH at 308 and 338 K in dry air atmosphere (in contact with silica gel as desiccant).

From the G'' curve (first run) a T_g of 274 K can be determined. (Slight deviations in the second run can be attributed to subtle changes of the crystallinity of the sample.) This value of T_g corresponds to the onset of the shift to lower relaxation rates in PPgMAH (Figure 4b) and therefore confirms the suggested correlation between local rearrangements affecting the dielectric behavior of the grafted MAH groups and cooperative segmental motions of the polymer. For both nanocomposite materials a T_g of 275 K was determined from G''.

4.3. Gravimetric Experiments: PPgMAH. The presence of polar groups (maleic anhydride) in the polymeric matrix leads to the presumption that water sorbed from the ambient atmosphere may cause the unusual relaxation behavior of PPgMAH. Effects of even low moisture contents on molecular relaxation processes have been discussed for other polymeric systems.[32−34]

4.3.1. Gravimetry: Dry Atmosphere. For a first proof of this presumption a film sample (about 100 mg) of PPgMAH was placed in a hermetically sealed microbalance system. The air atmosphere inside the microbalance was in contact with dry silica gel as desiccant. Therefore, the mass change of the sample resulting from the loss of water in dry air atmosphere could be recorded. Figure 6 shows the observed mass loss in two steps at 308 K (4 days) and 338 K (2.5 days).

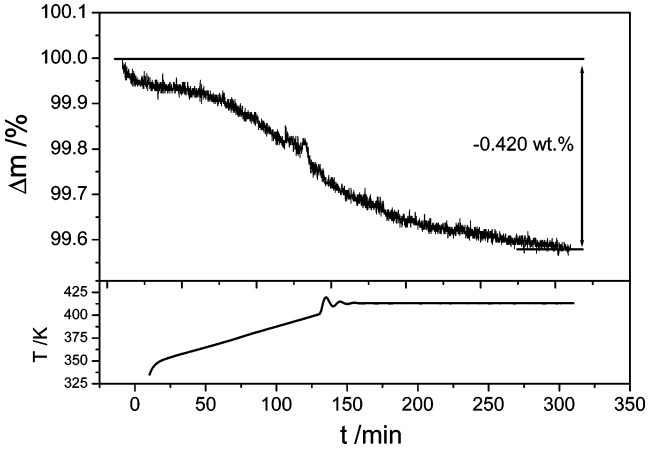

Figure 7. Weight change Δm (TGA) of PPgMAH during heating from ambient conditions (298 K) to 413 K and isothermal annealing at 413 K.

After 4 days at 308 K under dry conditions a mass decrease of 0.055 wt % was found; after about 2 more days at 338 K under the same conditions a further decrease of 0.090 wt % was detected. So a loss of water of about 0.14 wt % could be estimated under these conditions.

4.3.2. Thermogravimetric Analysis: PPgMAH. To get a more quantitative estimate of the water content in the PPgMAH samples the weight loss upon heating was investigated using thermogravimetric analysis (TGA) with heating rates of 5 K/min (303−353 K), 0.5 K/min (353−413 K), and isothermal conditions at 413 K (180 min) under nitrogen flow. In this temperature range no thermal degradation of the sample material could be observed, and the weight changes are fully reversible on a time scale of several hours under a moist air atmosphere. The observed weight change under these heating conditions (Figure 7) leads to an estimated loss of water of about 0.4 wt %. The significantly higher value of desorbed water under heating conditions (TGA) compared to the gravimetric experiments at 308 and 338 K in contact with a desiccant can be attributed to an enhanced diffusivity at elevated temperatures as well as to changes of the thermodynamic equilibrium of bonded water molecules in the polymeric matrix at higher temperatures, which were also revealed by the Raman spectroscopic investigations (cf. section 4.4).

4.4. Raman Spectroscopy: PPgMAH. To further verify the assumption of water being the reason for the unusual dielectric relaxation behavior, Raman scattering was employed. A comparison of the Raman spectra of PPgMAH and pure polypropylene (PP) is shown in Figure 8.

A peak in the Raman spectrum corresponding specifically to the grafted maleic anhydride groups could not be detected due to their low concentration in the polymeric matrix. One of the major differences of the PPgMAH spectrum is an intensive scattering background over the whole range from 1000 to 4000 cm^{-1} as well as a sharp OH peak at 3614 cm^{-1}. The latter can be assigned to "bonded" water molecules whereas the intensive scattering background can be attributed to water molecules more freely dispersed in the polymer matrix. To check the influence of elevated temperatures on this OH peak, the PPgMAH sample was heated to 333 K and kept there for 60 min, and subsequently, Raman spectra were recorded every few minutes at room temperature under ambient conditions (Figure 9).

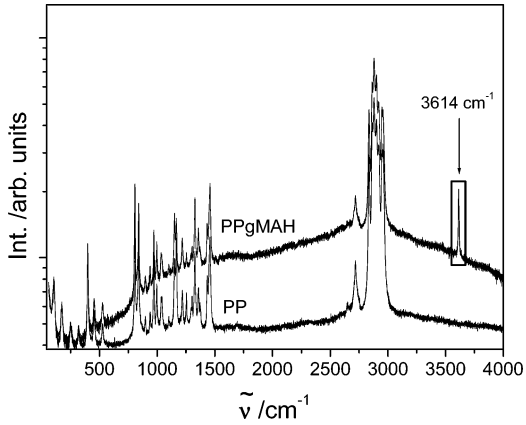

Figure 8. Comparison of Raman spectra of polypropylene (PP) and the matrix polymer PPgMAH (spectra represented to scale).

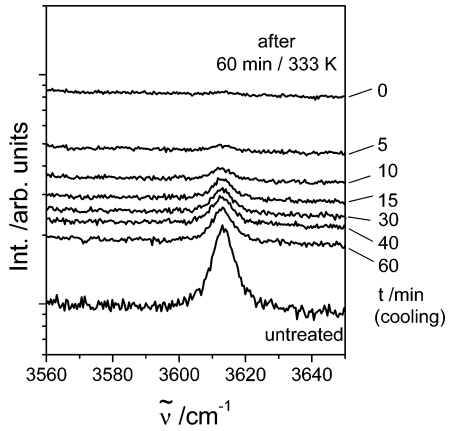

Figure 9. Raman spectra of PPgMAH, untreated, after 60 min of annealing at 333 K and reappearance of the OH peak during cooling at ambient conditions (spectra represented to scale).

It can be seen that the distinct peak at 3614 cm^{-1} vanishes completely after heating and then builds up again under ambient conditions (temperature, moisture) to reach the initial level again. At the same time the scattering background (represented to scale in Figure 9), which is further elevated after heating, is reduced during this period and also returns to its initial level. On the basis of this observation, it can be assumed that this behavior represents a shift of the concentration equilibrium between localized "bonded" water molecules, giving rise to the sharp peak at 3614 cm^{-1}, and water molecules which are more freely dispersed in the polymer matrix, causing the massive increase of the scattering background. This change of the respective intensities is reversible on a time scale of several hours. The return to the initial state at room temperature is slower than the change caused by the increase of temperature because an activated diffusion process of water molecules in the polymer matrix is involved which is significantly accelerated at higher temperatures.

4.5. Real-Time DRS under Controlled Atmospheres: PPgMAH. The results presented above suggest the existence of a hydratization shell around the maleic anhydride groups in the PPgMAH matrix polymer. Deriving a more detailed picture of these structures based on the results presented above seems too speculative since it cannot be expected that the estimation of water content is sufficiently quantitative, and furthermore additional information about formation of

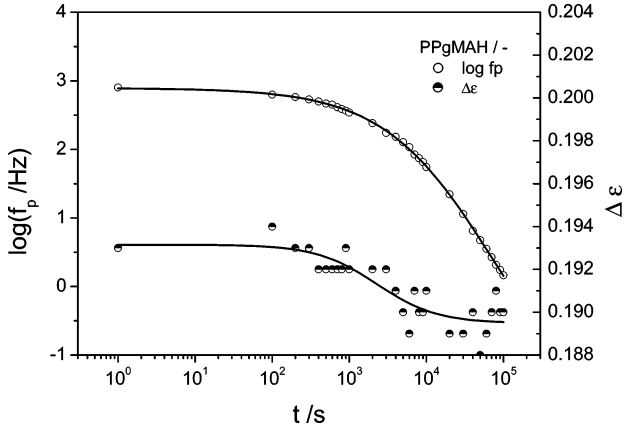

Figure 10. Relaxation rate (f_p) and dielectric relaxation strength ($\Delta\epsilon$) of PPgMAH upon evacuation from ambient conditions (real-time DRS at 298 K).

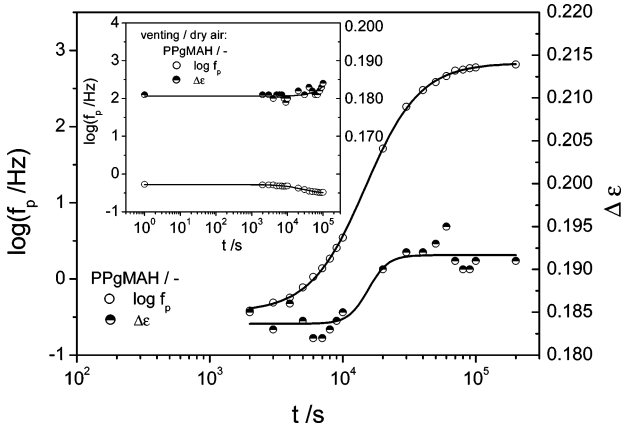

Figure 11. Relaxation rate f_p and dielectric relaxation strength $\Delta\epsilon$ of PPgMAH upon venting with moist air after evacuation (real-time DRS at 298 K). Inset: venting with dry synthetic air.

clusters or agglomerates of the polar MAH groups in the hydrophobic PP matrix would be necessary. The water molecules located in the vicinity of the MAH-groups may influence their dielectric relaxation behavior in two ways: (1) the mobility of the fluctuating polar units (MAH + bonded water) as well as (2) the effective dipole moment of these units should depend significantly on the number of water molecules and their local arrangement. Therefore, it can be expected that the dielectric relaxation time (corresponding to f_p) as well as the dielectric relaxation strength $\Delta\epsilon$ changes with the content and the distribution of water molecules in the polymer matrix. As shown in Figure 4b for PPgMAH the dielectric relaxation strength $\Delta\epsilon$ changes simultaneously to the beginning shift of the relaxation frequency f_p to lower values at temperatures above 293 K, which indicates a change of both mobility and effective dipole moment of the fluctuating molecular unit due to a rearrangement or loss of locally bonded water. At temperatures above 320 K there is no further decrease of $\Delta\epsilon$, but an increase vs $1/T$ with the same slope as below 293 K which again can be ascribed to an enhanced mobility of the surrounding matrix.

With regard to these findings it has to be noted that the experimental procedures established for the conventional DRS measurements in a dry nitrogen atmosphere are not designed to reliably characterize additional time-dependent phenomena such as the diffusion-controlled sorption and desorption of water. Neither a well-defined time regime nor an independent control of the water content of the sample or the surrounding atmosphere is possible.

A more direct way to characterize the influence of water molecules (and their redistribution) on the relaxation behavior are real-time dielectric measurements under controlled atmospheres. These experiments also allow a more quantitative assessment of this effect as the water concentration is affected directly by changes of the surrounding atmosphere or evacuation and not indirectly induced by temperature changes. Figure 10 shows the dielectric relaxation rate of the PPgMAH sample as a function of time during evacuation at room temperature (298 K).

The relaxation peak frequency observed for PPgMAH shifts by nearly 3 orders of magnitude to lower values upon evacuation. Similar to the conventional DRS measurements a simultaneous decrease of the dielectric relaxation strength $\Delta\epsilon$ of about 2% is observed. Because

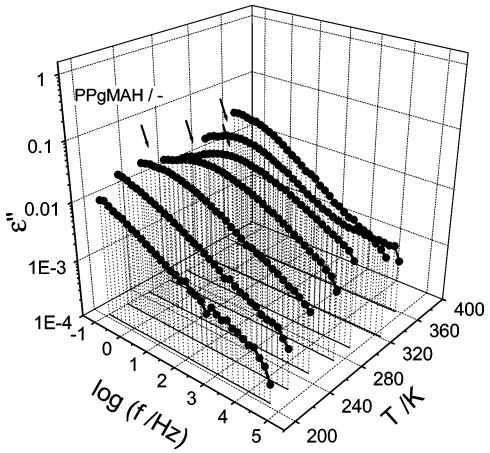

Figure 12. Dielectric loss ϵ'' of PPgMAH vs frequency at selected temperatures (conventional DRS) (arrows indicate the position of f_p).

the chemical structure of the polymer chains is not changed, obviously both effects have to be explained by a rearrangement or relocation of water molecules in the immediate environment of the maleic anhydride groups. This assumption is supported by additional real-time DRS experiments starting from the evacuated state of the PPgMAH sample. Following the measurement shown in Figure 10, the sample was first vented with dry synthetic air. As expected, no significant effect on f_p and $\Delta\epsilon$ was found (inset, Figure 11).

Subsequent venting with ambient moist air causes a shift of the relaxation peak back to higher frequencies as well as an increase of $\Delta\epsilon$. From the curves presented in Figure 11 it can be seen that both values reach their initial level after 12−24 h. It has to be noted that the kinetics of this process, which can be assumed to be due to a re-formation of a local water coordination shell in the vicinity of the maleic anhydride groups, is determined by diffusive transport of water molecules from the surrounding atmosphere into the material which is strongly affected by the geometry of the sample capacitor used for the dielectric experiments. As both surfaces of the sample film are covered by metal electrodes the sorption of moisture (as well as the desorption in the previous experiment) has to occur mainly by diffusion through its edges. It can be stated that the changes of the dielectric relaxation behavior revealed by real-time DRS measurements under controlled atmospheres are

caused by sorption/desorption of water molecules and prove to be reversible. The increasing temperature in the course of conventional DRS measurements, causing similar effects with regard to relaxation rate and dielectric relaxation strength, leads also to a shift in the water sorption equilibrium with the surrounding atmosphere. In this context it is obvious that the change in temperature may also give rise to local rearrangements of the coordination shell around the maleic anhydride in the polymer matrix, resulting in the observed dielectric response.

The observed changes in the Raman spectrum during a heating/cooling-cycle, as shown in Figure 9, and the DRS results discussed above both support the picture that changes in the local coordination with water molecules strongly influence the molecular mobility of the grafted maleic anhydride groups in the polypropylene matrix and that the presence of two populations of water molecules in the PPgMAH matrix polymer can be assumed: (1) localized water molecules leading to a sharp OH peak at 3614 cm^{-1} in the Raman spectrum and (2) water molecules more freely dispersed in the nonpolar polymer matrix giving rise to a distinct scattering background. The equilibrium between these two as well as with the water concentration in the surrounding gas phase are affected by the increasing temperature during conventional DRS and upon evacuation, revealed by corresponding real-time DRS measurements.

Compared to the results of conventional DRS measurements, the initial value of f_p observed in the real-time DRS experiments is distinctly higher. This has also to be attributed to changes in water content of the samples under respective measurement conditions. As the conventional DRS experiments start at 193 K, during initial cooling the sample is exposed to a dry nitrogen atmosphere for a certain time prior to the measurement. Also, the low-temperature frequency scans take several hours before 298 K, at which the time-dependent experiments were performed, is reached. So the material is exposed to an extremely dry atmosphere for a considerable time before the measurement at 298 K is performed, resulting in a reduced water content and a correspondingly lower mobility of the molecular dipoles. In contrast to this, the real-time DRS experiments start at the initial water content due to storage at ambient conditions.

4.7. Conventional DRS: Nanocomposites. Figures 13 and 14 show three-dimensional representations of selected dielectric loss curves (ϵ'') (Figures 13a and 14a) as well as relaxation rates f_p and dielectric relaxation strength $\Delta\epsilon$ vs $1/T$ (Figures 13b and 14b) for the nanocomposite materials containing Cloisite 30B and Nanomer I28E, respectively. For direct comparison, Figure 12 shows the dielectric loss of the pure PPgMAH matrix in the same three-dimensional style. For both clay composites conventional DRS measurements show the unusual temperature dependence as observed for unfilled PPgMAH: a decrease of f_p with increasing temperature above 293 K. In addition to the relaxation process caused by the localized fluctuations of the maleic anhydride groups, a separate high-temperature process can be observed which is considered to be caused by Maxwell−Wagner−Sillars polarization.[7,35]

For both PPgMAH/clay systems there is a linear shift of the relaxation peak with $1/T$ up to 293 K. The corresponding activation energies are quite similar to

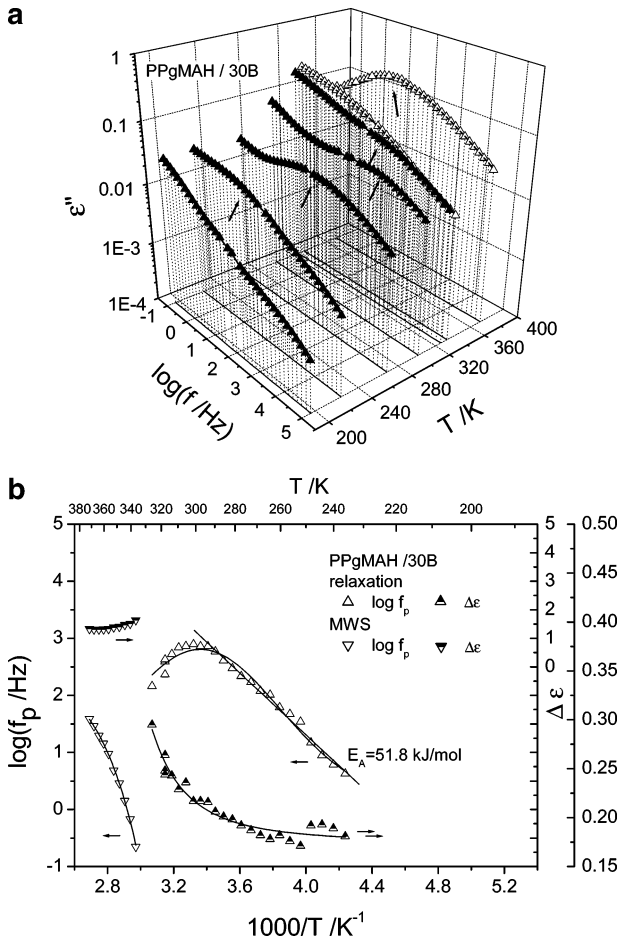

Figure 13. (a) Dielectric loss ϵ'' of the nanocomposite material PPgMAH/30B vs frequency at selected temperatures (conventional DRS, arrows indicate the position of f_p; solid symbols: molecular relaxation; open symbols: MWS polarization). (b) Relaxation rate f_p and dielectric relaxation strength $\Delta\epsilon$ of PPgMAH/30B vs $1/T$ (conventional DRS).

that in the unfilled polymer: slightly higher (51.8 kJ/mol) for the poorly dispersed PPgMAH/30B composite and a bit lower (46.8 kJ/mol) for PPgMAH/I28E, which is regarded as predominantly exfoliated clay nanocomposite. While for the pure polymer the analysis of the relaxation peak was possible also for temperatures above 293 K; in the composite materials the high-temperature process, with a higher dielectric loss, overlaps strongly the low-temperature relaxation process that the latter cannot be evaluated reliably at higher temperatures (see high-temperature curves indicated by open symbols in Figures 13a and 14a).

The high-temperature process can be clearly distinguished from the relaxation related to the maleic anhydride groups: the temperature dependence of its relaxation rate is significantly stronger (in the poorly dispersed composite even nonlinear), and the corresponding $\Delta\epsilon$ is more than 1 order of magnitude higher. Furthermore, it exhibits for both clay composite systems (see Figures 15 and 16) the characteristic strong increase of ϵ' with decreasing frequency of a Maxwell−Wagner−Sillars polarization which is caused by (partial) blocking of mobile charge carriers in inhomogeneous materials on a mesoscopic length scale (i.e., at internal boundary layers such as internal surfaces or interfaces). This leads to a separation of charges which give rise to a significant contribution to the polarization of the sample. The fact that using the same experimental

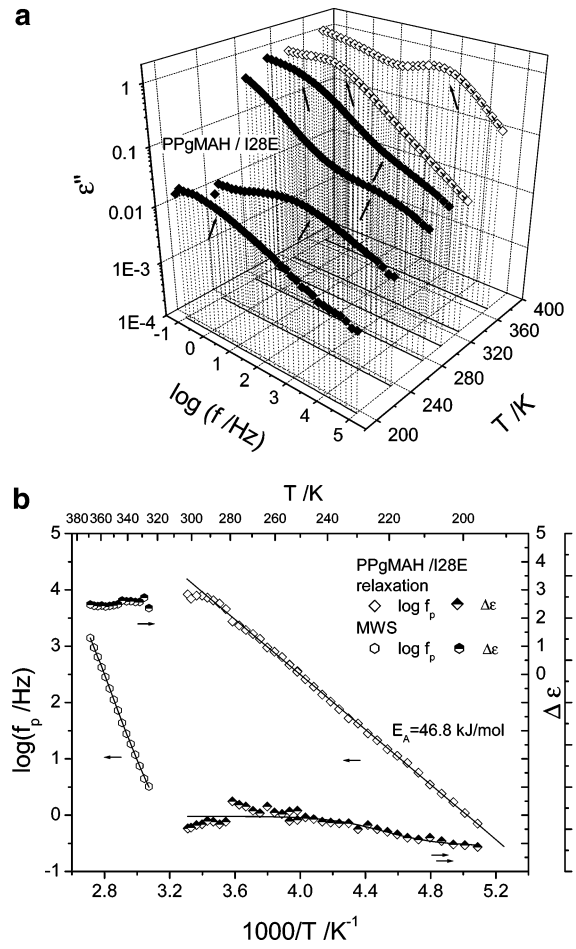

Figure 14. (a) Dielectric loss ϵ'' of the nanocomposite material PPgMAH/I28E vs frequency at selected temperatures (conventional DRS, arrows indicate the position of f_p; solid symbols: molecular relaxation; open symbols: MWS polarization). (b) Relaxation rate f_p and dielectric relaxation strength $\Delta\epsilon$ of PPgMAH/I28E vs $1/T$ (conventional DRS).

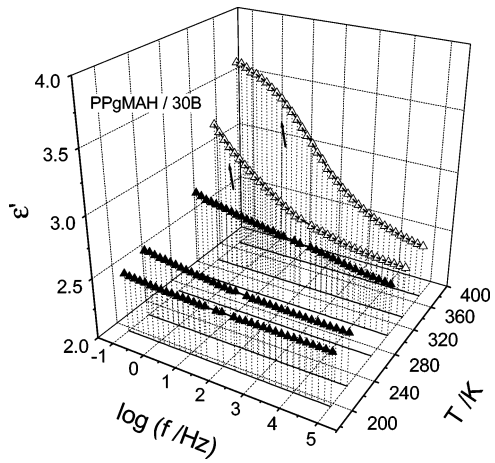

Figure 15. Dielectric permittivity ϵ' of PPgMAH/30B vs frequency at selected temperatures (conventional DRS) (arrows indicate the position of f_p of the MWS polarization; solid symbols: molecular relaxation; open symbols: MWS).

configuration (sample capacitor, film thickness) the frequency of maximal dielectric loss for the two nanocomposite materials differs significantly, and for the unfilled polymer no high-temperature process was observed, clearly excludes that the high-temperature process is caused by macroscopic electrode polarization.[7]

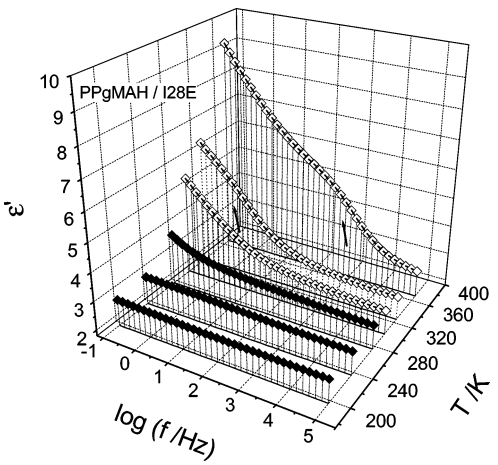

Figure 16. Dielectric permittivity ϵ' of PPgMAH/I28E vs frequency at selected temperatures (conventional DRS) (arrows indicate the position of f_p of the MWS polarization; solid symbols: molecular relaxation; open symbols: MWS).

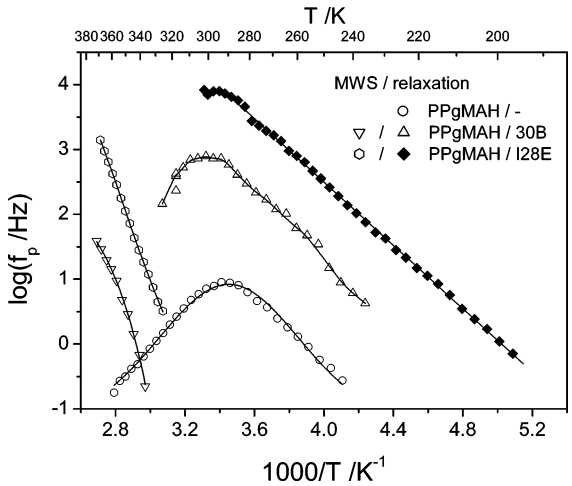

Figure 17. Frequency of maximal dielectric loss log f_p (relaxation and high-temperature process) of all investigated materials vs $1/T$ (conventional DRS).

Compared with the pure polymer the relaxation rates f_p for both clay composites (Figures 13 and 14) are distinctly shifted to higher values, especially in the case of the predominantly exfoliated nanocomposite PPgMAH/I28E. This indicates a significantly enhanced mobility of the molecular dipoles. For all three materials under investigation the maximum relaxation peak frequency is observed around 293 K but at different frequency levels, as shown in Figure 17.

On the basis of the results for the unfilled PPgMAH as well as for both nanocomposites discussed above, it can be assumed that the unusual decrease of f_p at temperatures above 293 K, corresponding to a decreasing molecular mobility of the polar MAH groups, has to be attributed to rearrangements and relocation of water molecules. As these phenomena have to be considered as diffusional processes they strongly depend on the dynamics of the polymer matrix. The obvious change of the water diffusivity (i.e., the mobility of water molecules within the polymer matrix) leading to the occurrence of such rearrangements in the temperature region above 293 K can therefore also be correlated with the glass transition of the PPgMAH matrix at 274 K (Figure 5).

The maximum value of log f_p for the unfilled PPgMAH is 1.0 while it is shifted to 3.0 and 4.3 for the clay-filled

system 30B and I28E, respectively. On the basis of the assumption that the grafted MAH groups (which solely give rise to the dielectric effects) are preferentially located at polymer/clay interfaces, it is concluded that the molecular mobility in these interfacial regions is enhanced. Apparently two possible reasons for this enhanced molecular mobility can be discussed: (1) the polymer/clay interface can induce changes in the local free volume distribution which may facilitate the fluctuation of the dipolar groups. Or it may also be possible that (2) the longer alkyl chains of the organophilic cations act as local plasticizers. Both arguments would also provide an explanation of the stronger mobility enhancement in the well-dispersed and predominantly exfoliated polymer/clay system which may be due to a larger fraction of internal interfaces or to a higher overall concentration of alkylammonium ions which are exposed to the surrounding matrix and not largely located within the clay galleries.

Although the separate high-temperature process due to Maxwell−Wagner−Sillars polarization observed in the dielectric spectra of the two nanocomposites prevents the analysis of the molecular relaxation process of the MAH groups at higher temperatures, it can provide further insight into the nanocomposite structure. Considering the layered geometry of the clay particles dispersed in the polymer matrix, the characteristic time of this process can be discussed in the framework of a simple model. The additional MWS polarization is caused by blocking of charge carriers at internal polymer/clay interfaces described by an electrical double layer with an effective spacing characterized by its Debye length L_D. This double layer represents an additional capacitance in the system, and the time dependence of the polarization is due to charging/discharging of that electrical double layer. Assuming a predominantly parallel orientation of partially delaminated/exfoliated silicate layers and a mean distance d between separated layers or stacks larger than L_D ($d \gg L_D$), the characteristic time $\tau_{MWS/clay}$ can be estimated in the simplest possible approach analogous to that for electrode polarization using eq 4[7]

$$\tau_{MWS/clay} = \frac{\epsilon_S \epsilon_0}{\sigma_0} \frac{d}{2L_D} \tag{4}$$

where ϵ_0 is the dielectric permittivity of vacuum and σ_0 is the dc conductivity of the system. The time constant $\tau_{MWS/clay}$ is therefore proportional to the mean distance between separated silicate layers in the nanocomposite materials.

$$\frac{\tau_1}{\tau_2} = \frac{f_{p,2}}{f_{p,3}} \approx \frac{d_1}{d_2} \tag{5}$$

The comparison of the relaxation rates f_p for the MWS processes in Figure 17 according to eq 5 reveals values for PPgMAH/I28E more than 1 order of magnitude higher compared to those for PPgMAH/30B; at 360 K f_p is 33 times higher, and at 340 K a factor of 45 can be deduced. This means that the mean distance between two separate silicate layers (or tactoids), causing the MWS polarization, is more than 30 times smaller in the well-dispersed nanocomposite than in the poorly dispersed PPgMAH/30B material. This finding is in agreement with the better dispersion of clay platelets in the PPgMAH/I28E nanocomposites as reported in ref 27 by

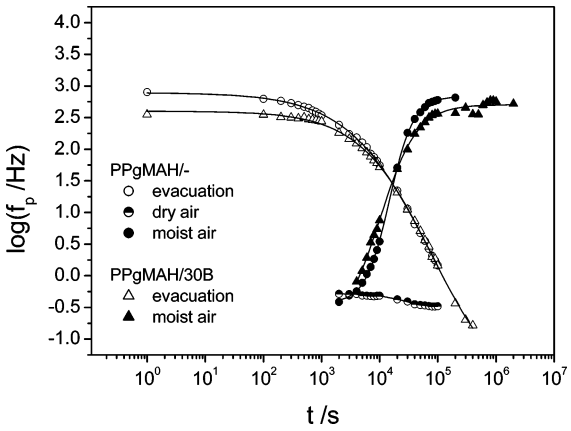

Figure 18. Relaxation rate f_p of PPgMAH and PPgMAH/30B upon evacuation and subsequent venting (real-time DRS).

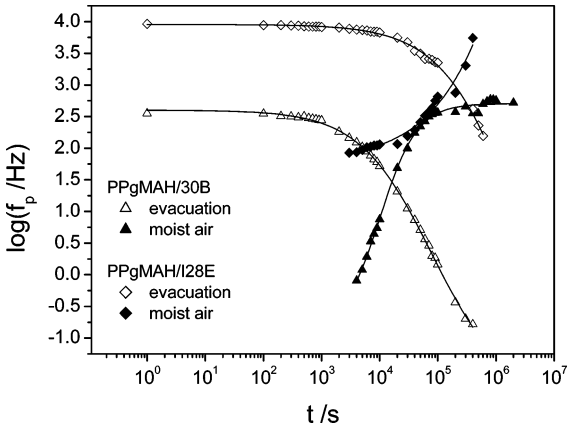

Figure 19. Relaxation rate f_p of PPgMAH/30B and PPgMAH/I28E upon evacuation and subsequent venting (real-time DRS).

Tidjani et al. Their TEM pictures (along with Figure 2 in this paper) and X-ray diffraction curves indicate that in the PPgMAH/30B material larger stacks (tactoids) of silicate layers dominate the composite morphology, whereas in the PPgMAH/I28E nanocomposites the higher degree of delamination or exfoliation of silicate layers leads to more homogeneously dispersed separated silicate layers, resulting in a smaller mean distance between polymer/clay interfaces.

4.8. Real-Time DRS under Controlled Atmospheres: Nanocomposites. Additional to the influence of sorbed water molecules in the PPgMAH/clay systems also the changes of the molecular mobility due to dispersion/exfoliation of the layered silicate fillers can be investigated in more detail by real-time dielectric measurements under controlled atmospheres.

The time dependence of f_p (shown in Figures 18 and 19) measured under vacuum conditions and venting with moist air, respectively, reveal significant differences for both systems. The poorly dispersed PPgMAH/30B material exhibits essentially the same behavior as the unfilled polymer, whereas the well-dispersed clay composite PPgMAH/I28E shows a significant shift to higher frequencies as well as a distinct slowdown of the desorption/sorption kinetics.

Under the isothermal conditions the poorly dispersed clay composite PPgMAH/30B and the unfilled PPgMAH exhibit a very similar behavior with respect to both the level of the observed molecular mobility and desorption/sorption kinetics. The shift to higher relaxation peak

frequencies observed for PPgMAH/I28E is in the same order of magnitude as observed by conventional DRS measurements although a quantitative comparison with the latter is not very reliable due to the experimental limitations concerning the actual water content at the time of measurement. As discussed above, changes in the local free volume distribution as well as the long alkyl chains of the organophilic clay cations may cause this locally enhanced mobility. The distinctly slower kinetic of the relaxation frequency shift clearly reflects the remarkable barrier properties of the exfoliated clay nanocomposite system (PPgMAH/I28E) which are predominantly due to more tortuous diffusion pathways caused by the impermeable silicate layers which are well dispersed within the polymer matrix.

5. Conclusions

The dielectrically active relaxation process in PPgMAH, which has to be assigned to localized fluctuations of the polar maleic anhydride groups, exhibits an unusual saddlelike temperature dependence, which obeys neither an Arrhenius nor a Vogel−Fulcher−Tammann law. Employing Raman spectroscopy and thermogravimetric experiments (TGA) in combination with real-time dielectric measurements under controlled atmospheres, it could be shown that this behavior is due to a redistribution of water molecules between a locally bonded state in the vicinity of the maleic anhydride groups and a more freely dispersion in the polymeric matrix. In the nanocomposites for this dielectrically active process relaxation rates up to 3 orders of magnitude higher than in the unfilled polymer were observed. Assuming that the maleic anhydride groups, which act as compatibilizers enabling the clay dispersion in the nonpolar matrix, are preferentially located in the interfacial regions between polymer and clay sheets or stacks (tactoids), this indicates a significantly enhanced molecular mobility in those regions. This enhanced molecular mobility may be attributed to an increase of local free volume or to plasticization by longer alkyl chains of the clay's organophilic cations. For an unambiguous differentiation between these two possible reasons much more comprehensive investigations would be necessary.

Real-time DRS furthermore reveals differences in the diffusivitiy of the water molecules reflecting the barrier effect of the clay platelets depending on their dispersion in the polymeric matrix and the degree of delamination or exfoliation.

For both nanocomposite systems a distinct high-temperature process was observed by DRS, which can be considered to be due to Maxwell−Wagner−Sillars (MWS) polarization. Corresponding relaxation rates allow a rough estimate of characteristic length scales in the nanocomposites and therefore also depend on the degree of dispersion of the filler particles (silicate layers). This correlation may provide a possible route for the development of testing or monitoring procedures in the field of nanocomposite formation although further investigations are required before practical applications are conceivable.

Both effects studied by DRS—local relaxation dynamics as well as MWS polarization—are able to provide valuable information on relevant bulk properties of polymer/layered silicate nanocomposites determined by structure formation and interfacial interactions on a nanometer scale.

Acknowledgment. The authors thank A. Tidjani for the preparation of the PPgMAH/clay nanocomposite films and M.-M. Pohl of ACA, Berlin, Germany, for the TEM investigation.

References and Notes

(1) LeBaron, P. C.; Wang, Z.; Pinnavaia, T. J. *Appl. Clay Sci.* **1999**, *15*, 11−29.
(2) Alexandre, M.; Dubois, P. *Mater. Sci. Eng.* **2000**, *28*, 1−63.
(3) Gilman, J. W. *Appl. Clay Sci.* **1999**, *15*, 31−49.
(4) Hartwig, A.; Pütz, D.; Schartel, B.; Bartholmai, M.; Wendschuh-Josties, M. *Macromol. Chem. Phys.* **2003**, *204*, 2247−2257.
(5) Bartholmai, M.; Schartel, B. *Polym. Adv. Technol.* **2004**, *15*, 355−364.
(6) Schmidt, D.; Shah, D.; Giannelis, E. P. *Curr. Opin. Solid State Mater. Sci.* **2002**, *6*, 205−212.
(7) *Broadband Dielectric Spectroscopy*; Kremer, F., Schönhals, A., Eds.; Springer: Berlin, 2002.
(8) Utracki, L. A.; Simha, R.; Garcia-Rejon, A. *Macromolecules* **2003**, *36*, 2114−2121.
(9) Hu, X.; Zhang, W.; Si, M.; Gelfer, M.; Hsiao, B.; Rafailovich, M.; Sokolov, J.; Zaitsev, V.; Schwarz, S. *Macromolecules* **2003**, *36*, 823−829.
(10) Böhning, M.; Hofmann, D.; Paul, D. In *Scientific Computing in Chemical Engineering II-1. Computational fluid dynamics, reaction engineering, and molecular properties*; Springer: Berlin 1999.
(11) Hofmann, D.; Fritz, L.; Ulbrich, J.; Schepers, C.; Böhning, M. *Macromol. Theory Simul.* **2000**, *9*, 293−327.
(12) Proceedings of the 2nd International Workshop on Dynamics in Confinement, *Eur. Phys. J. E* **2003**, *12*, 1−194.
(13) Kuppa, V.; Foley, T. M. D.; Manias, E. *Eur. Phys. J. E* **2003**, *12*, 159−165.
(14) Merkel, T. C.; Freeman, B. D.; Spontak, R. J.; He, Z.; Pinnau, I.; Meakin, P.; Hill, A. J. *Science* **2002**, *296*, 519−522.
(15) Merkel, T. C.; Freeman, B. D.; Spontak, R. J.; He, Z.; Pinnau, I.; Meakin, P.; Hill, A. J. *Chem. Mater.* **2003**, *15*, 109−123.
(16) Lu, H.; Nutt, S. *Macromolecules* **2003**, *36*, 4010−4016.
(17) Mahajan, R.; Koros, W. J. *Ind. Eng. Chem. Res.* **2000**, *39*, 2692−2696.
(18) Bur, A. J.; Roth, S. C.; McBrearty, M. *Rev. Sci. Instrum.* **2002**, *73*, 2097−2102.
(19) Bur, A. J.; Roth, S. C.; McBrearty, M. *Antec 2003* **2003**, 3326−3330.
(20) Davis, R. D.; Gilman, J. W.; Bur, A. J.; McBrearty, M.; Start, P. R.; Lee, Y.-H. *Polym. Mater. Sci. Eng.* **2004**, *90*, 715−716.
(21) Wagener, R.; Reisinger, T. J. G. *Polymer* **2003**, *44*, 7513−7518.
(22) Bourbigot, S.; Vanderhart, D. L.; Gilman, J. W.; Awad, W. H.; Davis, R. D.; Morgan, A. B.; Wilkie, C. A. *J. Polym. Sci., Part B: Polym. Phys.* **2003**, *41*, 3188−3213.
(23) Manias, E.; Touny, A.; Wu, L.; Strawhecker, K.; Lu, B.; Chung, T. C. *Chem. Mater.* **2001**, *13*, 3516−3523.
(24) Reichert, P.; Hoffmann, B.; Bock, T.; Thomann, R.; Mülhaupt, R.; Friedrich, C. *Macromol. Rapid Commun.* **2001**, *22*, 519−523.
(25) Anastasiadis, S. H.; Karatasos, K.; Vlachos, G.; Manias, E.; Giannelis, E. P. *Phys. Rev. Lett.* **2000**, *84*, 915−918.
(26) Kanapitsas, A.; Pissis, P.; Kotsilkova, R. *J. Non-Cryst. Solids* **2002**, *305*, 204−211.
(27) Tidjani, A.; Wald, O.; Pohl, M.-M.; Hentschel, M. P.; Schartel, B. *Polym. Degrad. Stab.* **2003**, *82*, 133−140.
(28) Vaia, R. A.; Jandt, K. D.; Kramer, E. J.; Giannelis, E. P. *Macromolecules* **1995**, *28*, 8080−8085.
(29) Fischer, H. *Mater. Sci. Eng. C* **2003**, *23*, 763−772.
(30) Schönhals, A.; Kremer, F. In *Broadband Dielectric Spectroscopy*; Kremer, F., Schönhals, A., Eds.; Springer: Berlin, 2002; Chapter 1.
(31) Schönhals, A. In *Broadband Dielectric Spectroscopy*; Kremer, F., Schönhals, A., Eds.; Springer: Berlin, 2002; Chapter 7.
(32) Cendoya, I.; Lopez, D.; Alegria, A.; Mijangos, C. *J. Polym. Sci., Part B: Polym. Phys.* **2001**, *39*, 1968−1975.
(33) Grimau, M.; Laredo, E.; Perez , M.C.; Bello, A. *J. Chem. Phys.* **2001**, *114*, 6417−6425.
(34) Mijovic, J.; Zhang, H. *Macromolecules* **2003**, *36*, 1279−1288.
(35) Perrier, G.; Bergeret, A. *J. Appl. Phys.* **1995**, *77*, 2651−2658.

MA048315C